Simulation and Optimization of Von-Mises Stress and Tip Deformation for Single Point Cutting Tool Geometry during Turning

Ashish Soni [1,*], Pankaj Kumar Das [1], Mohammad Yusuf [2,3,*], Hesam Kamyab [4,5], Mohammad Azad Alam [6], Moinul Haq [7], Yassine Ezaier [8], and Hussameldin Ibrahim [2]

[1] Centre for Additive Manufacturing, Chennai Institute of Technology, Chennai, Tamil Nadu, 600069, India
[2] Clean Energy Technologies Research Institute (CETRI), Process Systems Engineering, Faculty of Engineering & Applied Science, University of Regina, 3737 Wascana Parkway, SK, S4S 0A2, Canada
[3] Centre of Research Impact and Outcome, Chitkara University Institute of Engineering and Technology, Chitkara University, Punjab, India
[4] Department of Biomaterials, Saveetha Dental College and Hospital, Saveetha Institute of Medical and Technical Sciences, Chennai 600077, India
[5] The KU-KIST Graduate School of Energy and Environment, Korea University, 145 Anam-Ro, Seongbuk-Gu, Seoul, 02841, Republic of Korea
[6] Interdisciplinary Research Centre for Sustainable Energy Systems (IRC-SES), King Fahd University of Petroleum and Minerals (KFUPM), 31261, Dhahran, Saudi Arabia
[7] Interdisciplinary Research Center for Construction and Building Materials (IRC-CBM), Research Institute, King Fahd University of Petroleum & Minerals, Dhahran, 31261, Saudi Arabia
[8] Bio-Geosciences and Materials Engineering Laboratory, Ecole Normale Supérieure, University Hassan II, Casablanca, Morocco
Email: ashishsoni@citchennai.net (A.S.); researchnita2019@gmail.com (P.K.D.); mohd.yusuf@uregina.ca (M.Y.); hesam_kamyab@yahoo.com (H.K.), mohammad.alam@kfupm.edu.sa (M.A.A.), mohdmoinul.haq@kfupm.edu.sa (M.H.), yassine.ezaier14@gmail.com (Y.E.), hussameldin.ibrahim@uregina.ca (H.I.)
*Corresponding author

***Abstract*—The study aimed to quantify the values of von-mises stress and tip deformation of single point cutting tools of different tool geometries. Pro e Creo 5.0 was used for modeling the cutting tools and simulations were carried out through ANSYS 14.5. Three different materials for cutting tools namely, Cubic Boron Nitride (CBN), High-Speed Steel (HSS), and Gray cast iron having rake angles in the range of 1º–6º, 10º–15º and 20º–25º, respectively were taken for analyses. The rake angles were varied with a unit increment under the considered ranges with corresponding edge radii of 0.25, 0.20, 0.15, 0.10, 0.05, and 0.01 mm for each tool material. The cutting force was constant at 100 N considering engineering stress. The cutting speed of 2.54 m/s and a feed rate of 0.25 mm/revolutions were taken for the simulations of the cutting tool models. The minimum von-mises stress and tip deformation for CBN, HSS, and gray cast iron cutting tools were obtained at an edge radius of 0.15 mm having rake angles of 3º, 12º, and 22º, respectively. The resulted values have provided an estimation for von-mises stress and tip deformation thereby, assisting in improving the machinability, saving energy requirements, and preventing tool failures.**

***Keywords*—von-mises stress, simulation, finite element, tool geometry, single point cutting tool, machinability**

I. Introduction

Metal cutting forms the basis of the manufacturing process which generates the anticipated dimensions of the work piece by eliminating the excess materials as chips [1]. Single point metal cutting tools are widely used by varieties of metal cutting devices, including lathes and shaping machines. When the metal moves about the tool, a chip is torn off by the wedge-shaped pointed part of the tool, which exerts significant pressure on the work piece [2, 3]. It is crucial that machining tool must be of proper materials and cutting angles for effective metal cutting. The design and proper selection of the tool which has its own geometry had a significant impact on the machining procedure [4]. With the increasing demand for higher productivity, there is an urge for various technological operations such as the selection of work pieces, tool materials, optimal technological processes, and cutting sizes [5–7]. The tool geometry is one of the important machining variables that must be taken into account during machining to achieve the desired tool performance and process reliability [8–10]. Tool geometry and tool material are the significant factors that influence

Manuscript received November 4, 2024; revised November 28, 2024, accepted December 17, 2024; published March 26, 2025.

the machinability and performance [11–13]. The tool's performance was estimated by the reduction in stresses and greater stability to produce the desired shape [14, 15]. In the past, several conventional deterministic prediction techniques were often used to predict the forces however, due to the wide range of cutting parameters only sub-optimal solutions were possible to obtain [16–18]. Despite various available optimization techniques, there is no single general technique that can give the optimal value based on the input parameters and is equally applicable to all types of manufacturing processes [19–22]. The available optimization approaches are subjected to constraints and limitations that require certain assumptions for implementations in real problems [23]. Tool geometry is one of the key elements in determining the effectiveness of manufacturing processes is the tool geometry, which has historically been determined using projective geometry [24]. The cutting tool geometry has been specified by a number of standards, including the International Standard for Standardization (ISO), American Standards Associations (ASA), Deutsches Institute for Normung (DIN), and British Standard (BS) [25]. In the past few decades, the field of modeling and simulation through computer technologies has developed rapidly, and finite element analysis has emerges as one of the most widely used techniques for simulation [26–29].

The majority of earlier studies, however, concentrated on how machinability is influenced by tool parameters and chip formation and do not provide any explanation of how the tool geometry effect the material removal [30, 31]. In the present study, tool parameters namely rake angles and edge radius are examined for von-mises stress and tip deformation in a single point cutting tool during machining. The present work quantifies the von-mises stresses and tip deformation in orthogonal machining assuming a steady-state process where the removal of material from the work piece (elastic-viscoplastic) takes in the form of chips with inertia and damping effects. For each model, an explicit dynamic analysis is carried out on a stiffness matrix according to given conditions. The matrices are aggregated and the rigidity matrix of the system is generated. The modeling of single point cutting tools is carried out by using Pro e creo 5.0, and simulations are performed through ANSYS 14.5. The models of cutting tools having different geometries are obtained by varying the rake angle and edge radius for the three different materials namely, CBN, HSS, and Gray cast iron. Here, for each tool material there are six different models making a total of eighteen different models of cutting tools. The developed tools modes were individually simulated under a constant cutting force of 100 N taking into account the technical load with cutting speed and feed rate of 2.54 m/sec and 0.25 mm/rev., respectively. The simulation results provide an insight into how the von-mises stress and tip deformation are affected by tool geometry. The analysis of the results establishes that the tool geometry has a substantial effect on the thrust components and provides a better understanding which serves as the basis for an optimal tool geometry to prevent tool failures and provides a direction for future research by considering the other elements of tool geometry with different tool materials.

II. Literatures

The researchers have worked to estimate the value of cutting force under the different tool geometries by using ANSYS [32]. Patel *et al.* [33] have proposed a computational system for harmonic analysis to reduce the chattering in a single point cutting tool during turning. Bhogal *et al.* [34] have performed the analysis for thermal and cutting force to improve the machinability of the carbide tool while turning 4140 alloy steel. Mishra *et al.* [35] have developed an alternative conjugate approach for heat transfer measurement through computational methods. The model can calculate the temperature of any profile by several numerical equations. Choudhari *et al.* [36] have employed ANSYS to analyze the vibration and deformation of a tool for different nose radii and tool materials. The obtained results were imported to Minitab through the design of experiments to generate a regression equation. Pervaiz *et al.* [37] have estimated the distribution of heat in a cutting tool and coefficient of heat transfer through the integration of computational fluid dynamics and finite elements. Kohli *et al.* [38] have carried out the analysis of heat in a cutting tool coated with naturally obtained biocomposite. Tripathi *et al.* [39] have applied finite elements to determine the harmonic response analysis of a tool coated with epoxy-granite in different ranges. Nikam *et al.* [40] have evaluated the performance of a with different textures. Moreover, the effect of stress on tool wear and tool life was studied through a model based on 3D finite element. The study has predicted the temperature of the carbide tool [41]. Meng *et al.* [42] have demonstrated the explicit kinetic simulation of a saw blade on the basis orthogonal test in finite elements. Keuntje *et al.* [43] have developed a simulation model which works on micro levels to realize the distribution of temperature in a cutting tool during the removal of materials.

III. Statement of Problem

The cutting forces and power requirement depend upon the rake angle which can be negative, zero, or positive. In practice, it has been observed that the tool forces reduce with an increase in rake angle [44]. Furthermore, it is reported that tool life decreases with the rake angle whereas the forces across the tool decrease with the rake angle [45]. Rake angle is significant for proving the shear plane which reduces with rake angle consequently, the required forces [46]. However, the tool with higher positive rake angles has lower mechanical strength which reduces tool life. The rake angle has shown their dependency on the work piece and tool material, the machine setup, and the machining process. The edge radius is another geometric parameter that determines the strength of the tooltip, feed rate, and quality of the finished surface [47]. A tool with a greater edge radius is stronger as compared to a tools with a smaller radius as it offers better failure safety (chipping or breaking) and surface quality at a given feed rate [48]. Whereas, tool with a small

edge radius are required as the cutting forces are always perpendicular to the cutting edge with a greater edge radius and more force are encountered to the work piece and tool. This is particularly a problem in case of smaller cutting depth which leads to deflection of the part and/or tool deflection unlimitedly results in tapered cuts, chatter, poor finish and possible breakage. The edge radius should be sufficient to sustain the cutting effect but beyond a certain limit, it reduces the stress concentration. Furthermore, von-mises is the combination of three principal stresses which is responsible for the failure or fracture of the tools. The earlier studies have revealed that the tool parameters influence the tool life [49, 50]. ANSYS 14.5 provides a general-purpose, automated, intelligent meshing software with high performance to create accurate and efficient solutions ranging from simple to highly engineered networks. The accuracy, convergence and speed of the simulation are influenced by the number of elements, the larger the number more precise will be the result.

In the present work, the dependency of the two geometrical parameters, namely rake angle and edge radius are considered to select a suitable combination of rake angles and edge radius for a cutting tool to reduce the effect of vibration on the cutting material for desired surface finish and prevents the tool failure also decrease the overall cost of production. To achieve this ANSYS simulations are considered suitable for evaluations of von-mises stresses and tip deformations. Table I shows the recommended values of rake angles. The novelty of the research can be given in four folds (i) optimization of cutting tools performances by taking the two geometrical parameters, simultaneously (ii) a wide of tool and work piece materials (iii) simulations of eighteen different sets of tools (iv) implementation of two cutting-edge techniques for optimizations of tool performances.

TABLE I. RAKE ANGLES FOR TOOL AND WORK PIECE MATERIAL

S. No.	Cutting tool material	Work piece material	rake angle
1.	CBN	Inconel	1º–8º
2.	HSS	Mild Steel 1090	12º–14º
3.	Gray cast iron	Aluminium alloy AA5754	12º–25º

IV. TOOL MODELING

The cutting tool is modeled by using Pro e creo 5.0. The 3D models are then imported into the ANSYS 14.5 workbench for simulations by a GUI command. Figs. 1 and 2 show the geometrical parameters and prepared model of the cutting tool, respectively with details of the dimensions given in Table II.

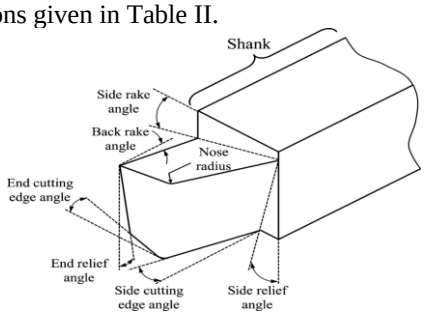

Fig. 1. Geometry of single point cutting tool.

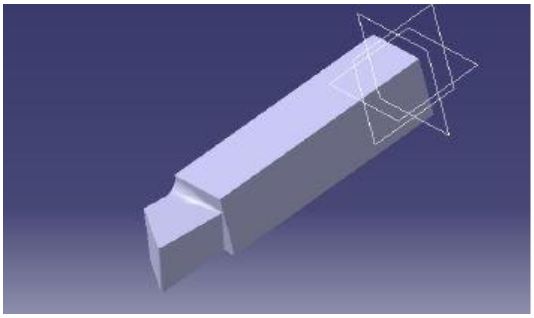

Fig. 2. Model of single point cutting tool.

TABLE II. GEOMETRICAL PARAMETERS OF SINGLE POINT CUTTING TOOL

S. No.	Parameters	Value
1.	Back rake angle	1º–6º (For CBN) 8º–15º (For mild steel) 20º–25º (For Gray cast iron)
2.	Side rake angle	12º
3.	End relief angle	10º
4.	Side relief angle	5º
5.	End cutting edge angle	30º
6.	Side cutting edge angle	15º
7.	Edge radius	0.25–0.01 mm

V. MECHANICAL CUTTING

Mechanical cutting obtains the required shape due to the cutting action by using a single point or multipoint cutting tool. The tools having a single cutting edge are termed single point cutting tools and found their applications on lathes, shaping and slotting machines. Rake angle effects the tool deformation and temperature in steady state condition as well as the tool stress. Furthermore, cutting force increases with tedge radius [51]. Discontinuous chips are obtained at lower rake angle, the adiabatic shear has been highlighted as the prominent factor as it removes the chip surface to retain the maximum heat [52]. The application of an external force either to the tool or work piece produces a relative movement and formation of the shear zone. The tool deformation is localized in the shear zone which initiates chip formation. The shearing action generates heat and increases the temperature of the cutting tool, work piece, and chips. The elevated temperature causes the softens the tool tip to soften and leads to deformation [53]. The tip deformation depends on the contact length, cutting force and friction force [54]. Fig. 3 given below shows the classical model of orthogonal cutting.

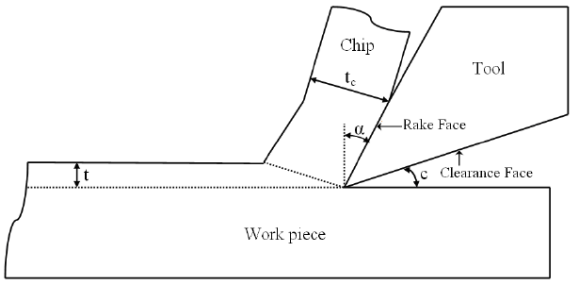

Fig. 3. Classical model of orthogonal cutting.

VI. Tool-Chip Inference

During machining the cutting forces act over a small area on the rake face which is termed as tool-chip interface [55]. The chip flows over the rake face and then curves away. The qualitative examination of the tool-chip interface enables the proper assortment of tool material and geometry. The shear stress, normal force and mean normal stress at the tool-chip interface are the characteristics of a tool-chip interface. The analysis of the stress shows the presence of plastic and elastic zones. The contact length decreases with the rake angle which increases the stresses. The decrease of mean shear stress at elevated temperature is fulfilled by stress and consequently, the strain rate therefore maintains a constant stress. The stresses increase with hardness and decrease with the rake angle [56]. Here, the chip formation mechanism is obtained by considering the cutting tool as a rigid body while the work piece is modeled as a deformable body. Initially, the tool is on the right of the work piece as the tool advances the crack generates according to the surface crack mechanism extends to the cutting edge and stops somewhere inside the chip due to excessive compression. The presence of cracks can be understood by the mechanism of chip formations [57]. The formation of continuous, segregated and discontinuous chips is observed in various tool models with different geometries. Moreover, at 15º of the rake angle continuous chips with little segmentation are obtained. The segregated chips are observed in the middle range of rake angles which is analogous to the observations in the present work [58].

VII. Analytical Calculation of Stresses and Tip Deformation

Analytically the stress (σ) of the cutting tool is calculated by using the rake angle ($\boldsymbol{\alpha}$) and chip thickness ratio ($\boldsymbol{r}$) as follows:

$$Shear\ angle\ (\varphi) = \frac{r cos\boldsymbol{\alpha}}{1 - r sin\boldsymbol{\alpha}}$$

$$Normal\ force\ (F_N) = F_c \sin\varphi\ + F_t \cos\varphi$$

$F_c = Cutting\ force$
$F_t = Thrust\ force$
$Stress\ (\sigma) = \frac{F_n}{A_s}$
A_s= $Shear\ area$

Von-mises (σ_m) is used for the prediction of failure of a material. It is a combination of three principal stresses into an equivalent stress and is given by the equation.

$$\sigma_m = \sqrt{\frac{\left[\left(\sigma_x - \sigma_y\right)^2 + \left(\sigma_y - \sigma_z\right)^2 + (\sigma_z - \sigma_x)^2\right]}{+3(\tau_{xy}^2 + \tau_{yz}^2 + \tau_{zx}^2)}}$$

$\sigma_x = normal\ stress\ in\ x\ direction$
$\sigma_y = normal\ stress\ in\ y\ direction$
$\sigma_z = normal\ stress\ in\ z\ direction$
$\tau_{xy} = shear\ stress\ in\ x - y\ direction$
$\tau_{yz} = shear\ stress\ in\ y - z\ direction$
$\tau_{zx} = shear\ stress\ in\ z - x\ direction$

The forces acting on the tool from the work piece causes the deformation of tip in a single point cutting tool. The tip deformation is calculated according to the Castigliano theorem which stated that the deformation is equivalent to the derivative of strain energy against the forces and is given by the below equation.

$$^{\delta} = uF_c$$

$^{\delta} = tip\ deformation$
$u = strain\ energy$
$F_c = cutting\ force$

VIII. Experimental Procedure

3D models of single point cutting tools of three different materials namely cubic boron nitride, high-speed steel and gray cast iron are selected. The geometries of tool models are varied by changing the rake angle and edge radius. The 3D models of the individual single point cutting tools are created in Pro e creo 5.0. Further simulations are carried out by using ANSYS 14.5 whereby a constant cutting force of 100 N is used for the simulations of the tool models. The cutting speed and feed rate are 2.54 m/s and 0.25 mm/rev., respectively. The results of the simulations are important to obtain an optimal tool geometry. The models of the cutting tools are prepared by using the selected parameters and imported into ANSYS 14.5 workbench for meshing which divides a model into a finite number of small elements and simulations. The basic steps for meshing are shown in Fig. 4. The present work considers free meshes for simulations of the cutting tool with an element size of 0.9 mm having 4494 nodes and 3474 elements. The cutting force is taken as 100 N considering engineering stress with cutting speed and feed rate of 2.54 m/s and 0.25 mm/rev. respectively for simulations of all models. The work piece is applied with fixed support to the bottom and the cutting tool is moved towards the work piece in the x-direction taking an end time of 1 s. The prepared models for cutting tools having different rake angles and edge radii are simulated for the von-mises stress and tip deformation to obtain appropriate combinations of the geometrical parameters (rake angle and edge radius) which lead to minimal values for von-mises and tip deformation within the available sets of tool geometries for the given tool materials. Table III illustrates the mechanical properties of the cutting tool, and the work piece used for simulations.

Fig. 4. Steps for meshing in ANSYS 14.5 workbench.

TABLE III. MECHANICAL PROPERTIES OF TOOLS AND WORK PIECE MATERIALS

S. No.	Material	Properties					
		Hardness	Coefficient of linear expansion at 20 ℃ (µm/m/K)	Young's Modulus (GPa)	Yield Strength (MPa)	Failure stress (MPa)	Melting temp. (℃)
1.	CBN (cutting tool)	660 HV	3.7	195	575	454	2973
	Inconel (work piece)	335 HV	12.8	207	980	1375	1336
2.	HSS (cutting tool)	458 HV	12.3	190	380	450	1430
	Mild steel 1090 (work piece)	140 HV	11.1	210	247	841	1530
3.	Gray cast iron (cutting tool)	210 HV	9	90	276	276	1300
	Aluminium Alloy AA5754 (work piece)	33.3 HV	23	69	90	280	660

IX. RESULT AND DISCUSSIONS

CBN is a hard material having hardness comparable to diamond. It has a higher heat diffusion capacity as compared to carbide and high speed steel, and is less reactive than diamond. CBN tools are mainly used for machining ferrous metals such as cast iron, titanium etc. [59]. CBN is stable at high temperatures up to 1000 ℃ and is generally achieved while machining hardened ferrous or superalloy materials. CBN cutting tools permit machining at a greater depth of cut and feed rate at a higher speed than conventional cutting tool materials. CBN tools can also be used for interrupted machining. Finite element simulations are carried out for a single point cutting tool made of Cubic Boron Nitrite (CBN) for machining of Inconel as work piece material. The CBN tool material has a modulus of elasticity of 195 GPa, a poisson's ratio of 0.3, and yield strength of 575 MPa. The ranges for rake angles used for CBN cutting tools are 1º–6º with unit increments for each model and corresponding edge radii of 0.25, 0.20, 0.15, 0.10, 0.05, and 0.01 mm respectively. The different sets for rake angles and edge radius for the CBN cutting tool are listed in Table IV. All the models of cutting tools are modeled in Pro e creo 5.0 and then imported into ANSYS 14.5 workbench in IGES format for simulations. The simulations for von-mises stress and the tip deformation are shown in Fig. 5 (a)–(f). The resulting values of the von mises stress and tip deformation for CBN tool material are listed in Table V. From the obtained results for CBN tools, it is observed that the von-mises stress and tip-deformation increases with rake angle from 1º to 2º and attains a maximum value of von-mises stress and tip deformation at rake angle of 2º then decreases irregularly which results in the minimum value of the von-mises stress and deformation to 1.0215e7 and 1.0866e−5, respectively with a rake angle of 3º therefore for CBN cutting tool rake angle of 3º and edge radius of 0.015 mm is suitable for machining of cast iron and titanium. The value of edge radius corresponding to the minimum value of von-mises stress and tip deformation for the CBN tool is 0.15 mm. Figs. 6 and 7 show the plots of von mises stresses and tip deformation, respectively among the given set of rake angle (º) and edge radius (mm). The plotted graphs clearly show the behavior of von-mises stress and tip-deformations varies with rake angle and edge radius. It is from the result analysis that tool geometry is a complex variable and finite element analysis is a suitable tool for simulation and quantifies the values of von-mises stresses and tip deformation.

TABLE IV. DIFFERENT SETS OF RAKE ANGLE AND EDGE RADIUS FOR CBN TOOL MATERIAL

S. No.	Rake angle	Edge radius
1	1º	0.25 mm
2	2º	0.20 mm
3	3º	0.15 mm
4	4º	0.10 mm
5	5º	0.05 mm
6	6º	0.01 mm

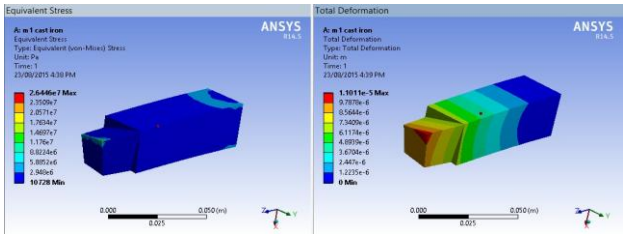

(a)

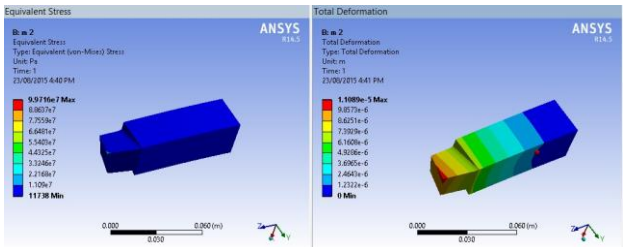

(b)

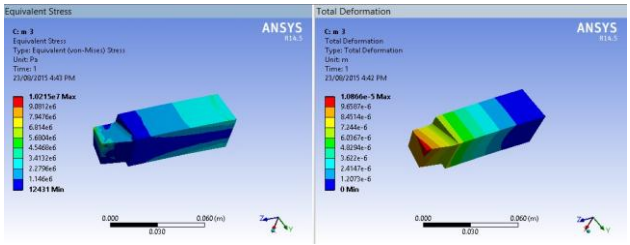

(c)

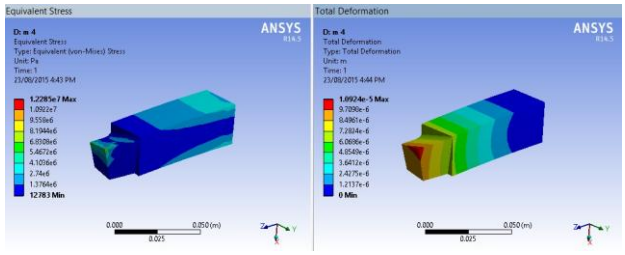

(d)

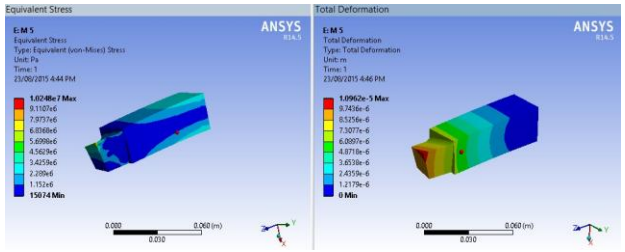

(e)

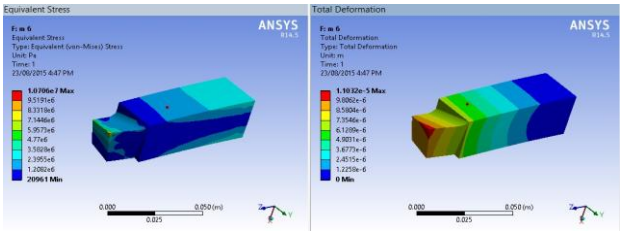

(f)

Fig. 5 (a). Stress and tip-deformation for rake angle 1º and edge radius 0.25 mm. (b). Stress and tip-deformation for rake angle 2° and edge radius 0.20 mm. (c). Stress and tip-deformation for rake angle 3° and edge radius 0.15 mm. (d). Stress and tip-deformation for rake angle 4° and edge radius 0.10 mm. (e). Stress and tip-deformation for rake angle 5° and edge radius 0.05 mm. (f). Stress and tip-deformation for rake angle 6° and edge radius 0.01 mm.

TABLE V. VON-MISES STRESS AND DEFORMATION OF CUBIC BORON NITRITE TOOL

S. No.	Rake Angle	Edge radius	Von Mises Stress (Pascal)	Tip Deformation (Meter)
1	1º	0.25 mm	2.6446e7	1.1011e−5
2	2º	0.20 mm	9.9716e7	1.1089e−5
3	3º	0.15 mm	1.0215e7	1.0866e−5
4	4º	0.10 mm	1.2285e7	1.0924e−5
5	5º	0.05 mm	1.0248e7	1.0962e−5
6	6º	0.01 mm	1.0706e7	1.1032e−5

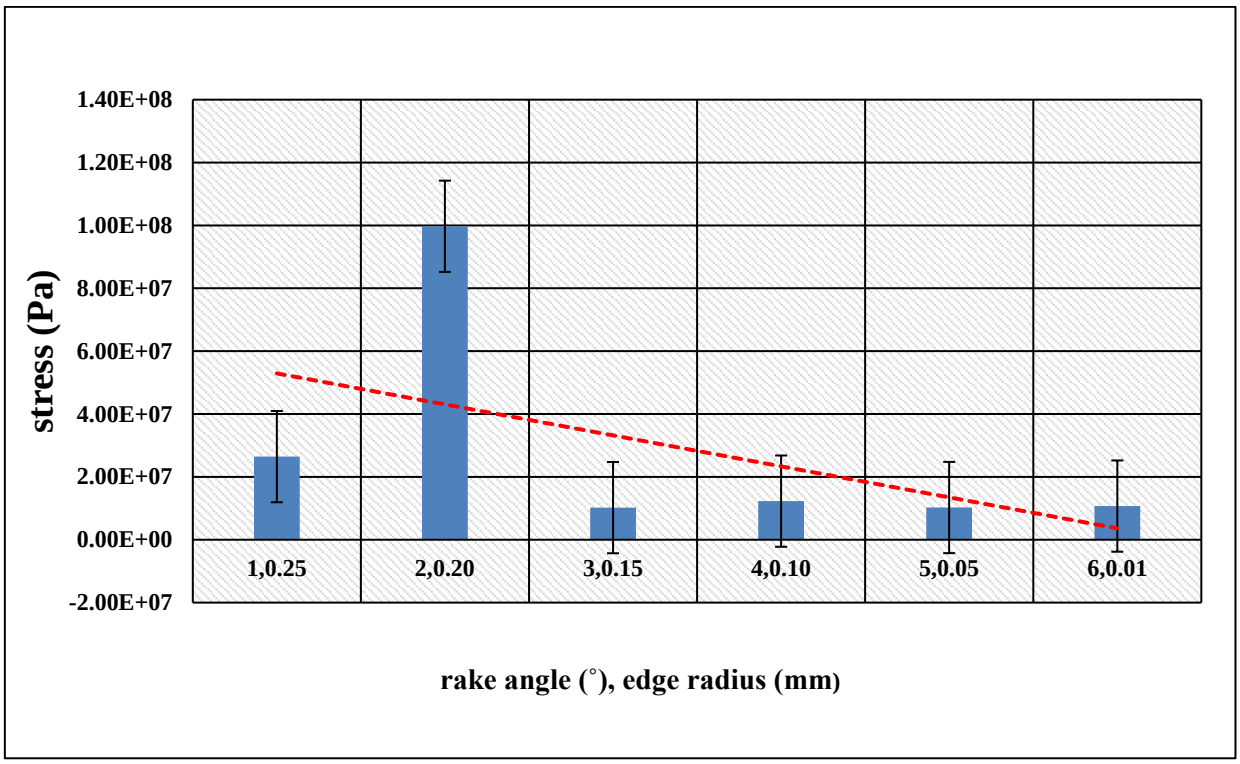

Fig. 6. Stress versus rake angle (º) and edge radius (mm).

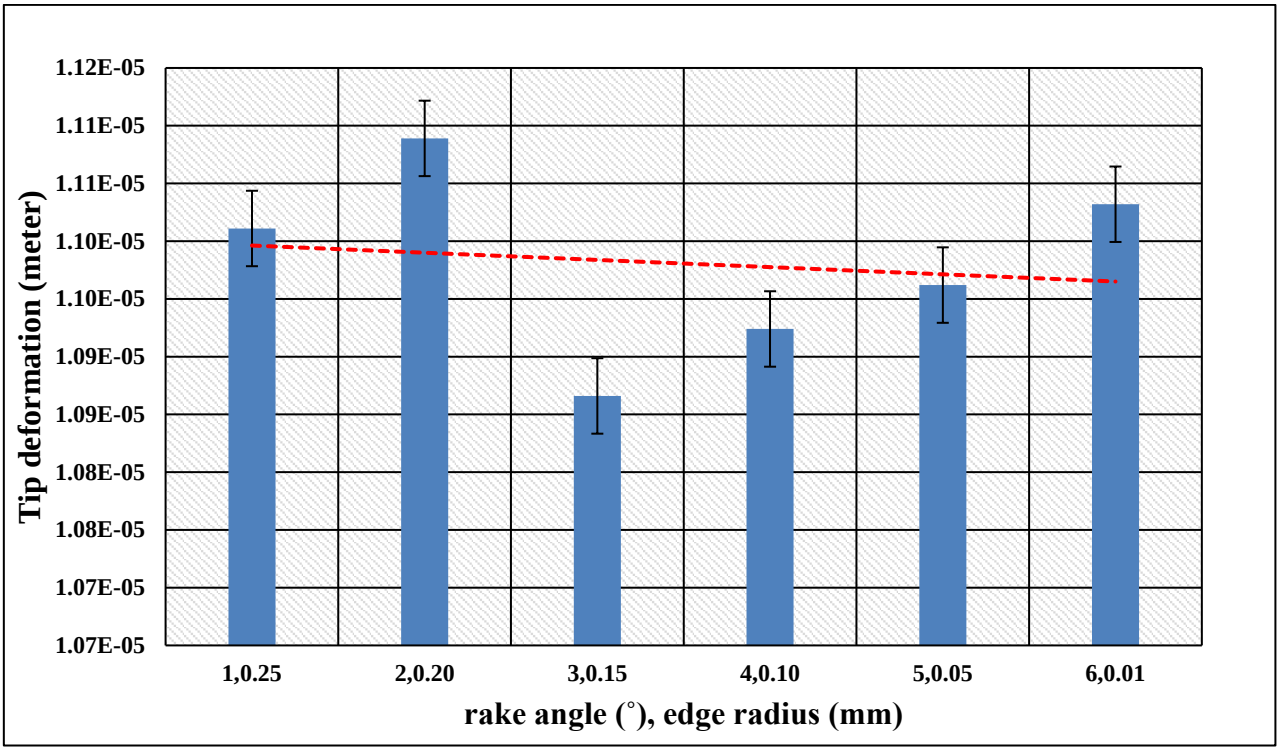

Fig. 7. Tip deformation (meter) versus rake angle (º) and edge radius (mm).

HSS was developed in the latter half of the nineteenth century and is quite suitable for cutting at higher speeds compared to carbon-cutting tools without losing their hardness [60]. It is a complex structured ferrous alloy with alloying elements that enables HSS tools for machining at higher speed than carbon tools. HSS tools retain their hardness up to 650 ℃ and are used for machining softer materials such as mild steel, brass, bronze, etc. The recommended range of rake angle for the HSS cutting tool is 8º–14º [61]. In the present simulations, the rake angles for HSS cutting tools vary from 10º to 15º for machining work pieces of mild steel. HSS has a modulus of elasticity of 190 GPa, poisson's ratio of 0.26, and yield strength of 380 MPa. The selected tool models are listed in Table VI. Fig. 8 (a)–(f) shows the simulations of von-mises stresses and tip-deformation for HSS tools obtained from ANSYS simulation. The resulted von-mises stress and tip deformation for high-speed steel cutting tool for the given set of rake angles and the edge are shown in Table VII. The obtained values for von-mises stress and tip deformation showed that the values decreases non-linearly and attain a minimum value of von-mises stress and deformation of the tip at a rake angle of 12º with a corresponding edge radius of 0.15 mm within the given set tool model and continue to increases. Figs. 9 and 10 show the values of von-mises stress and tip deformation for the tool models with different rake angles and edge radii. The graph behaves differently for the resulted values of von-mises stresses and tip deformation. The influence of other variables could be the possible cause for such nonlinear behavior.

TABLE VI. DIFFERENT SETS OF RAKE ANGLE AND EDGE RADIUS FOR HSS TOOL MATERIAL

S. No.	Rake angle	Edge radius
1	10º	0.25 mm
2	11º	0.20 mm
3	12º	0.15 mm
4	13º	0.10 mm
5	14º	0.05 mm
6	15º	0.01 mm

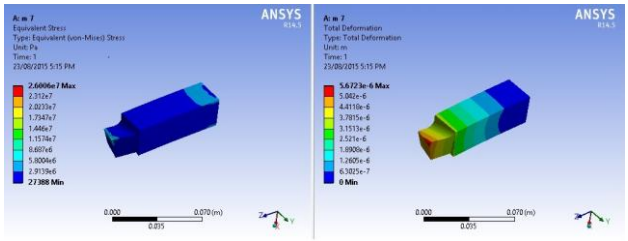

(a)

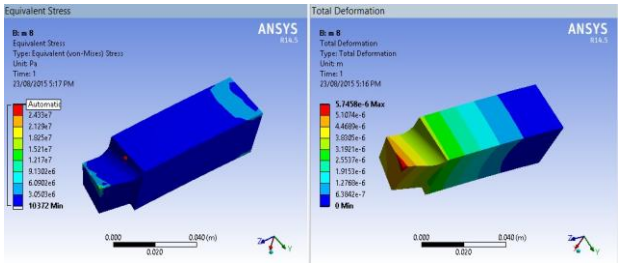

(b)

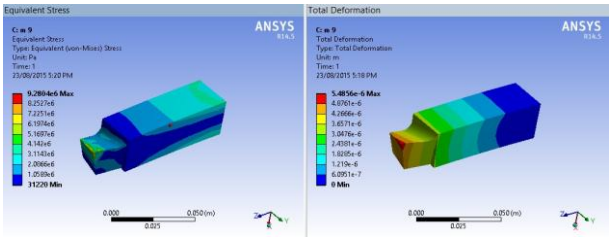

(c)

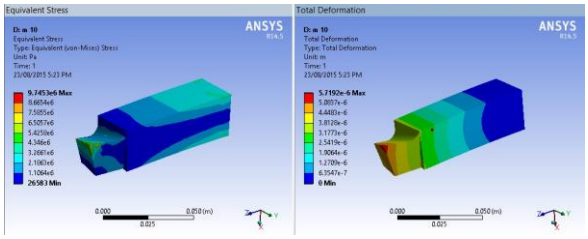

(d)

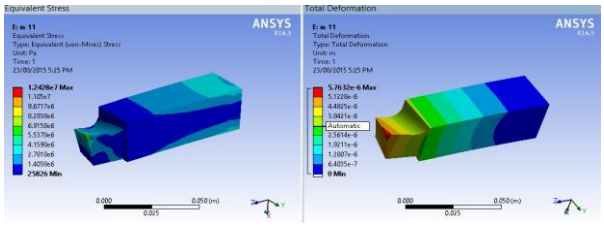

(e)

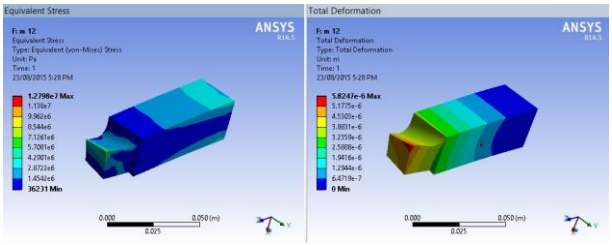

(f)

Fig. 8. (a). Stress and tip-deformation for rake angle 10° and edge radius 0.25 mm. (b). Stress and tip-deformation for rake angle 11° and edge radius 0.20 mm. (c). Stress and tip-deformation for rake angle 12° and edge radius 0.15 mm. (d). Stress and tip-deformation for rake angle 13° and edge radius 0.10 mm. (e). Stress and tip-deformation for rake angle 14° and edge radius 0.05 mm (f). Stress and tip-deformation for rake angle 15° and edge radius 0.01mm.

TABLE VII. VON-MISES STRESS AND TIP DEFORMATION OF HIGH SPEED STEEL

S. No.	Rake angle	Edge Radius	Von-Mises Stress (Pascal)	Tip deformation (Meter)
1	10º	0.25 mm	2.6007e7	5.6723e−6
2	11º	0.20 mm	2.7370e7	5.7458e−6
3	12º	0.15 mm	0.92804e7	5.4856e−6
4	13º	0.10 mm	0.97453e7	5.7192e−6
5	14º	0.05 mm	1.2428e7	5.7632e−6
6	15º	0.01 mm	1.2789e7	5.8247e−6

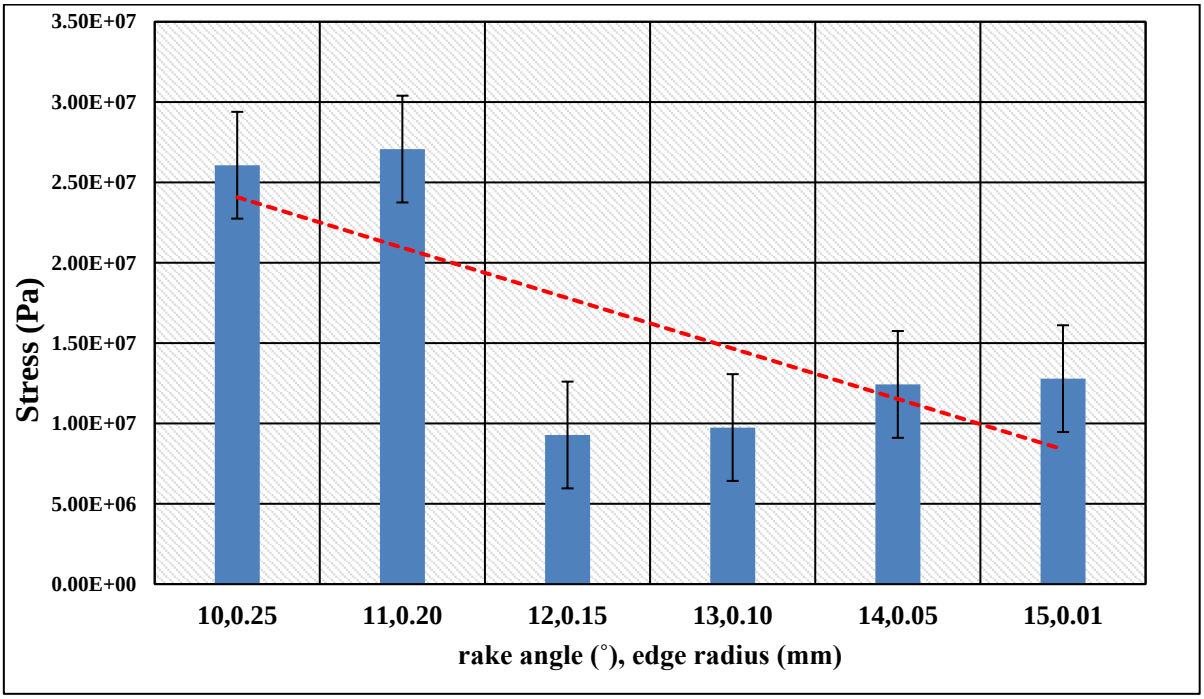

Fig. 9. Stress versus rake angle (º) and Edge radius (mm).

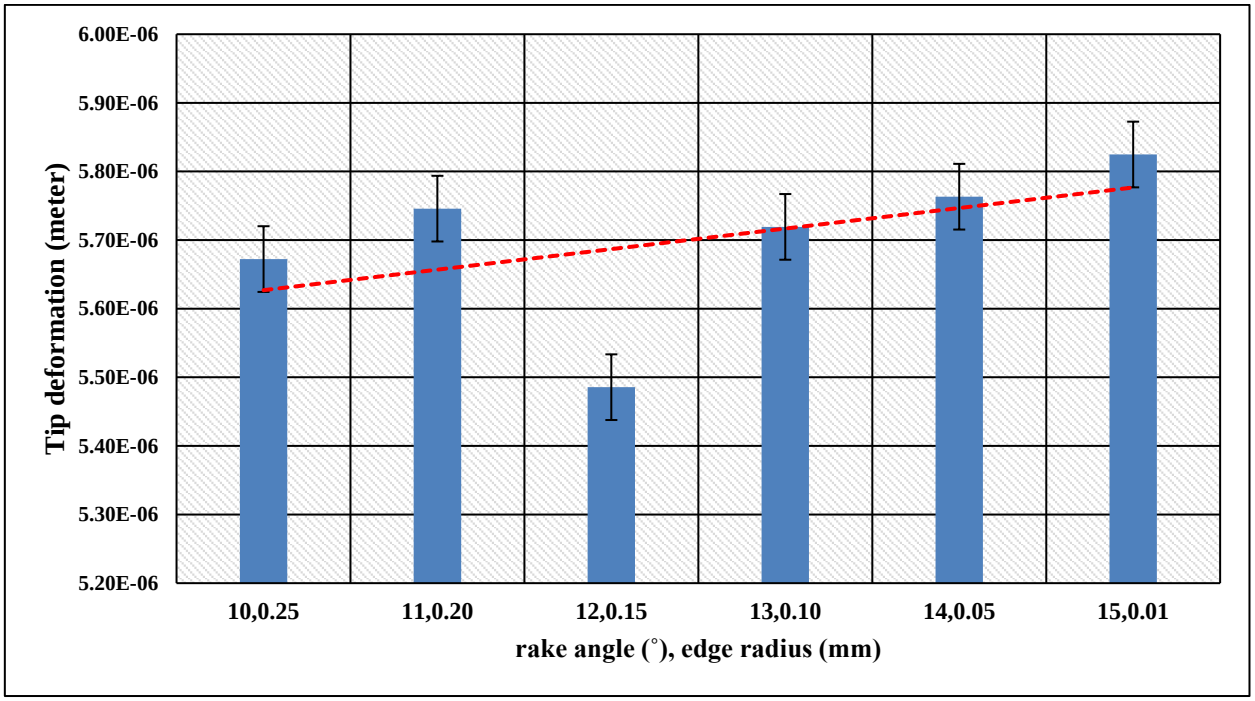

Fig. 10. Tip deformation (meter) versus rake angle (º) and edge radius (mm).

Gray cast iron has been widely used for cutting tool material since the 1880s. It is a type of cast iron having a graphitic microstructure. Grey cast iron loses its hardness at 250 °C as a result it can't be used in high-temperature applications making it an unsuitable material for cutting tools in modern machining operations. Gray cast iron is an inexpensive metal for cutting tools therefore, is used for low-machining operations. Materials such as Copper, Polyvinyl Chloride (PVC), and aluminum, etc. are easy to machine with gray cast iron cutting tools. The recommended range of rake angle while machining work piece of mild steel is 18º–25º [62]. In the present simulations, the rake angle is varied from 20º to 25º for the six different models listed in Table VIII. Gray cast iron is has a modulus of elasticity of 90 GPa, Poisson's Ratio of 0.22, and a yield strength of 276 MPa. Figs. 11 (a)–(f) shows the ANSYS simulations of the selected models. The obtained value for von-mises stresses and tip deformation for the models are shown in Table IX. The resulted values of von-mises stress and tip deformation illustrated that for grey cast iron the minimum value of von-mises stress and tip deformation is obtained at rake angle of 22º and edge radius of 0.15 mm. The obtained values of von mises and tip deformation are plotted against the rake angle and edge radius as shown in Figs. 12 and 13, respectively. The overall analysis of the von-mises stress and tip deformation of the different tool models of cubic boron nitride, high speed steel, and gray cast iron cutting tool materials at 100 N force with variable rake angle and edge radius showed that the developed models results in minimum values of the von mises stress for cubic boron nitride, high speed steel, and gray cast iron materials at an edge radius of 0.15 mm with rake angle 3º, 12º, and 22º, respectively.

TABLE VIII. DIFFERENT SETS OF RAKE ANGLE AND EDGE RADIUS FOR GRAY CAST IRON TOOL MATERIAL

S. No.	Rake angle	Edge radius
1	20º	0.25 mm
2	21º	0.20 mm
3	22º	0.15 mm
4	23º	0.10 mm
5	24º	0.05 mm
6	25º	0.01 mm

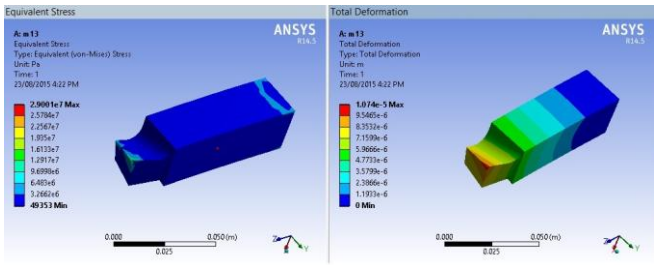

(a)

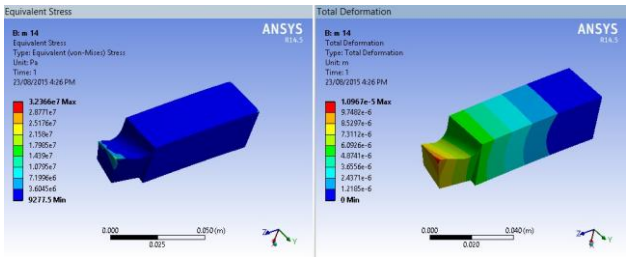

(b)

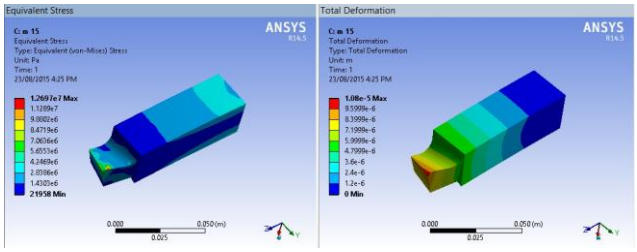

(c)

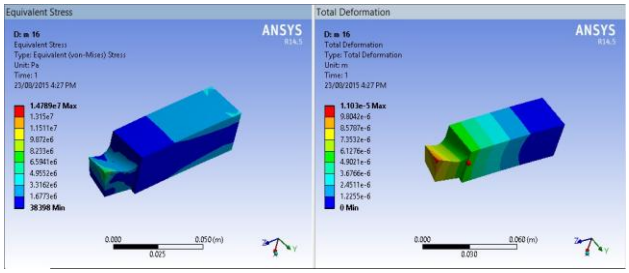

(d)

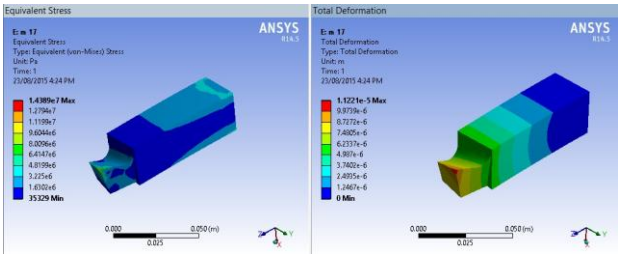

(e)

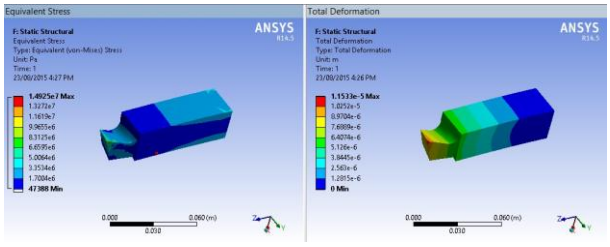

(f)

Fig. 11. (a). Stress and tip-deformation for rake angle 20° and edge radius 0.25 mm. Stress and tip-deformation for rake angle 21° and edge radius 0.20 mm. (c). Stress and tip-deformation for rake angle 22° and edge radius 0.15mm. (d). Stress and tip-deformation for rake angle 23° and edge radius 0.10 mm. (e). Stress and tip-deformation for rake angle 24° and edge radius 0.05 mm. (f). Stress and tip- for rake angle 25° and edge radius 0.01 mm.

TABLE IX. VON-MISES STRESS AND DEFORMATION OF GRAY CAST IRON TOOL

S. No.	Rake angle	Edge radius	Von Mises Stress (Pascal)	Tip Deformation (m)
1	20^0	0.25 mm	2.9001e7	1.074e−5
2	21^0	0.20 mm	3.2366e7	1.096e−5
3	22^0	0.15 mm	1.2697e7	1.080e−5
4	23^0	0.10 mm	1.4789e7	1.103e−5
5	24^0	0.05 mm	1.4389e7	1.122e−5
6	25^0	0.01 mm	1.4928e7	1.153e−5

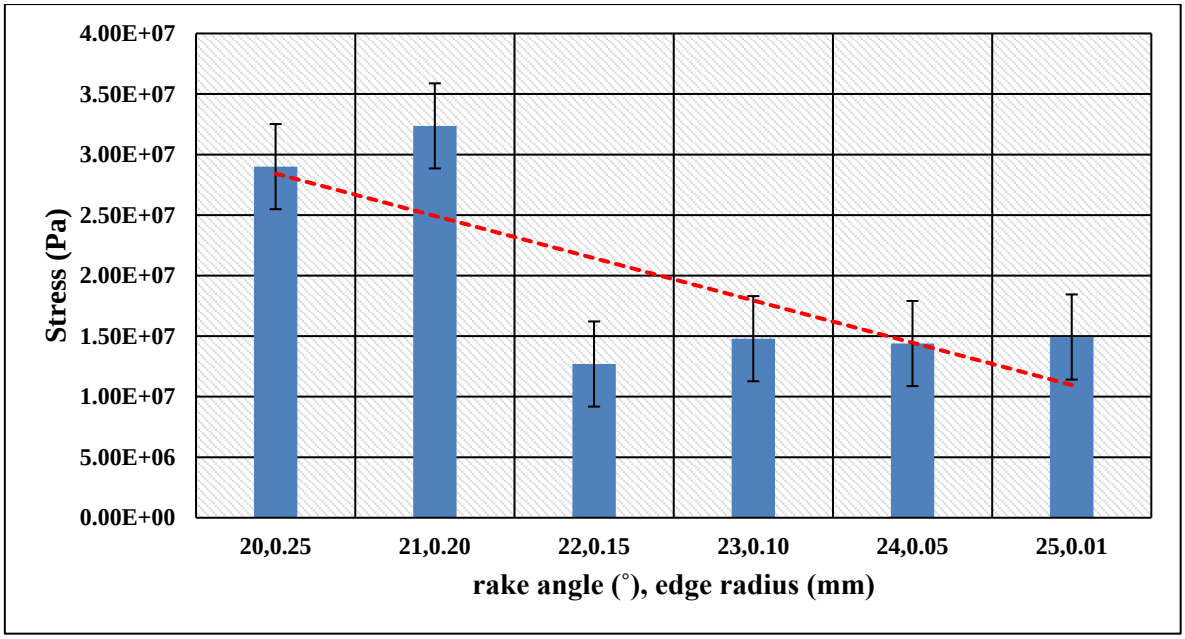

Fig. 12. Stress versus rake angle (º) and edge radius (mm).

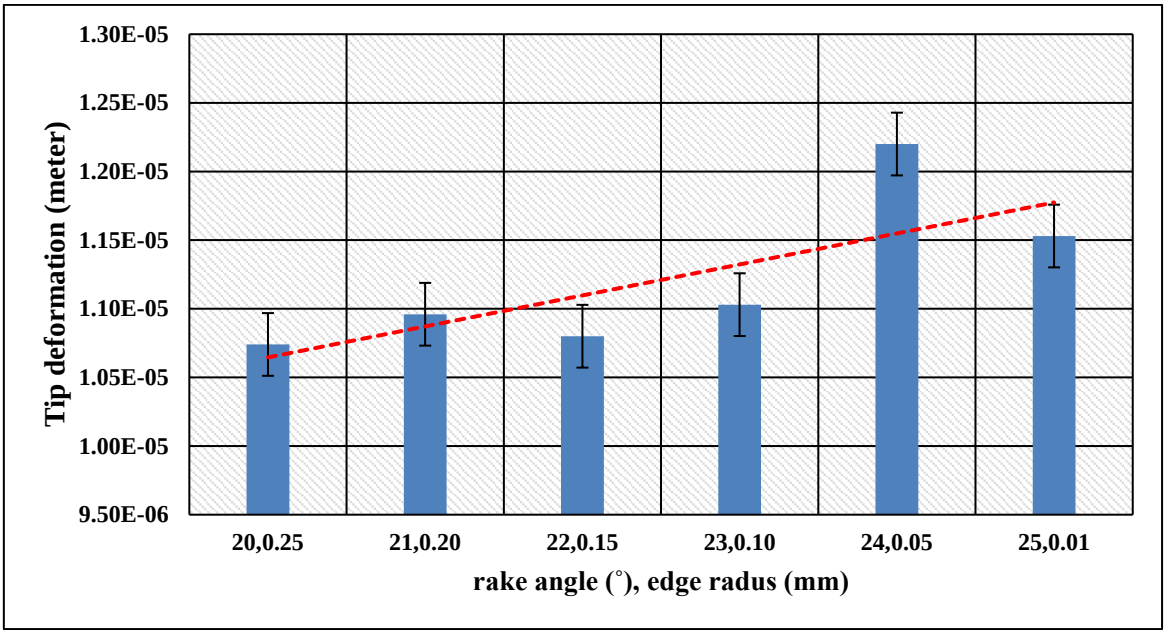

Fig. 13. Tip deformation (meter) versus rake angle (º) and edge radius (mm).

X. Conclusions

Cutting tool parameters are considered as the engine behind any manufacturing process which can be a single point cutting tool or a multiple point cutting tool. To meet the demand for higher productivity with accuracy and surface integrity a suitable tool geometry is required. The rake angle is one of the geometrical variables which affects the machinability of the work piece and tool performance i.e. tool life, cutting forces, surface finishing, etc. In the present research, Finite element analysis is used to simulate the tool models and analyze the influence of rake angle and edge radius on von-mises stresses and tip deformation which are cumbersome to predict experimentally. The obtained results have shown that von mises stress decreases non-linearly with an increase in the rake angle attains a minimum value then increases again. For the different sets of values for rake angles, and edge radius for cubic boron nitrate, high-speed steel and gray cast iron tool materials the minimum values of the von-mises stresses are obtained at rake angles of 3º, 12º and 22º, respectively at an edge radius of 0.15 mm. The simulation result has provided an understanding of the influences of the tools geometry on the von-mises stress and the tip deformation. It concludes that the von-mises stress encountered during machining and tip deformation influences with the tools geometry. An accurate estimation of the resulting stresses plays a pivotal role in preventing tool failures, reducing the production cost and improving machinability. The experimental validation of the research findings could be the future scope of the present work.

Data and Code Availability

The data that support the findings of this study are available on request from the corresponding author. The data are not publicly available due to privacy or ethical restrictions.

Conflict of Interest

The authors declare no conflict of interest.

Author Contributions

AS: Investigations, Writing—original draft, Writing—review & editing, Validation, Methodology, Visualization. PKD: Writing—review & editing, Supervision, Formal analysis, Resources, Data curation. MY: Writing—original draft, Writing-review & editing, Resources, Formal analysis. HK: Writing—review & editing, Formal analysis, Data curation. MAA: Visualization, Validation, Methodology. MH: Writing-review & editing, Formal analysis, Drafting. YE: Writing—review & editing, Data curation, Resources, Formal analysis, HI: Writing-review & editing. All authors had approved the final version.

Acknowledgment

The author would like to thank NIT Agartala, India, for providing resources in conducting this research.

References

[1] J. Ren, G. Zhang, Y. Rong, and Y. Ma, "A feature-based model for optimizing HVOF process by combining numerical simulation with experimental verification," *Journal of Manufacturing Processes*, vol. 64, pp. 224–238, 2021. https://doi.org/10.1016/j.jmapro.2021.01.017

[2] S. Prvulovic, P. Mosorinski, D. Radosav *et al.*, "Determination of the temperature in the cutting zone while processing machine plastic using Fuzzy-Logic Controller (FLC)," *Ain Shams Engineering Journal*, vol. 13, no. 3, 101624, 2022. https://doi.org/10.1016/j.asej.2021.10.019

[3] D. Dupláková, M. Hatala, J. Duplák *et al.*, "Illumination simulation of working environment during the testing of cutting materials durability," *Ain Shams Engineering Journal*, vol. 10, no. 1, pp. 161–169, 2019. https://doi.org/10.1016/j.asej.2018.10.004

[4] I. Alshalal, H.M.I. Al-Zuhairi, A. A. Abtan *et al.*, "Characterization of wear and fatigue behavior of aluminum piston alloy using alumina nanoparticles," *Journal of the Mechanical Behavior of*

Materials, vol. 32, no. 1, 20220280, 2023. https://doi.org/10.1515/jmbm-2022-0280

[5] D. M. Osborne and R. L. Armacost, "Review of techniques for optimizing multiple quality characteristics in product development," *Computers & Industrial Engineering*, vol. 31, no. 1–2, pp. 107–110, 1996. https://doi.org/10.1016/0360-8352(96)00089-7

[6] M. Adnouni, L. Jiang, X. Zhang *et al.*, "Computational modelling for decarbonised drying of agricultural products: Sustainable processes, energy efficiency, and quality improvement," *Journal of Food Engineering*, 111247, 2022. https://doi.org/10.1016/j.jfoodeng.2022.111247

[7] Z. He, H. Hu, M. Zhang *et al.*, "A decomposition-based multi-objective particle swarm optimization algorithm with a local search strategy for key quality characteristic identification in production processes," *Computers & Industrial Engineering*, 108617, 2022. https://doi.org/10.1016/j.cie.2022.108617

[8] R. Melentiev, P. C. Priarone, M. Robiglio, and L. Settineri, "Effects of tool geometry and process parameters on delamination in CFRP drilling: An overview," *Procedia Cirp*, vol. 45, pp. 31–34, 2016. https://doi.org/10.1016/j.procir.2016.02.255

[9] X. Soldani, C. Santiuste, A. Muñoz-Sánchez *et al.*, "Influence of tool geometry and numerical parameters when modeling orthogonal cutting of LFRP composites," C*omposites Part A: Applied Science and Manufacturing*, vol. 42, no. 9, pp. 1205–1216, 2011. https://doi.org/10.1016/j.compositesa.2011.04.023

[10] M. T. Ngo, "Effects of machining parameters on total cutting force in hard turning process of hardened 90CrSi steel using carbide insert with MoS2 nanofluid MQL," *International Journal of Mechanical Engineering and Robotics Research*, vol. 13, no. 1, 2024. doi: 10.18178/ijmerr.13.1.169-174

[11] M. S. M. Basri, M. Z. M. Nor, R. Shamsudin *et al.*, "Effects of different fluting medium geometries on von-mises stress and deformation in single fluted board: A three-dimensional finite element analysis," *Advances in Agricultural and Food Research Journal*, vol. 2, no. 1, 2021. https://doi.org/10.36877/aafrj.a0000138

[12] M. Ozakpolor and C. Aliyegbenoma, "Expert modelling and prediction of von mises stresses in high speed steel cutting tool using FEM (ANSYS)," *Academic Platform-Journal of Engineering and Science*, vol. 9, no. 3, pp. 397–402, 2021. https://doi.org/10.21541/apjes.741439

[13] L. M. Azaath, E. Mohan, and U. Natarajan, "Effect of rake angle and tool geometry during machining process of AISI 4340 steel in finite element approach," *Materials Today: Proceedings*, vol. 37, pp. 3731–3736, 2021. https://doi.org/10.1016/j.matpr.2020.10.196

[14] G. Skordaris, K.-D. Bouzakis, P. Charalampous *et al.*, "Effect of structure and residual stresses of diamond coated cemented carbide tools on the film adhesion and developed wear mechanisms in milling," *CIRP Annals*, vol. 65, no. 1, pp. 101–104, 2016. https://doi.org/10.1016/j.cirp.2016.04.007

[15] S. Dechjarern, "3D finite element investigations of the influence of tool rake angle on cutting performance," *Australian Journal of Mechanical Engineering*, vol. 7, no. 1, pp. 53–59, 2009. https://doi.org/10.1080/14484846.2009.11464578

[16] S. H. Din, N. Sheikh, and M. M. Butt, "Mechanical and tribological behavior of microcrystalline CVD diamond coatings," *Journal of Bio-and Tribo-Corrosion*, vol. 4, no. 2, pp. 1–10, 2018. https://doi.org/10.1007/s40735-018-0144-1

[17] K. Erkorkmaz, A. Katz, Y. Hosseinkhani *et al.*, "Chip geometry and cutting forces in gear shaping," *CIRP Annals*, vol. 65, no. 1, pp. 133–136, 2016. https://doi.org/10.1016/j.cirp.2016.04.040

[18] B. Denkena and D. Biermann, "Cutting edge geometries," *CIRP Annals*, vol. 63, pp. 631–653, 2014. https://doi.org/10.1016/j.cirp.2014.05.009

[19] N. H. Ononiwu, E. T. Akinlabi, and C. G. Ozoegwu, "Optimization techniques applied to machinability studies for turning aluminium metal matrix composites: A literature review," *Materials Today: Proceedings*, vol. 44, pp. 1124–1129, 2021. https://doi.org/10.1016/j.matpr.2020.11.228

[20] M. Akgün and F. Kara, "Analysis and optimization of cutting tool coating effects on surface roughness and cutting forces on turning of AA 6061 alloy," *Advances in Materials Science and Engineering*, vol. 2021, 6498261, 2021. https://doi.org/10.1155/2021/6498261

[21] B. R. Krishnan and M. Ramesh, "Optimization of machining process parameters in CNC turning process of IS2062 E250 Steel using coated carbide cutting tool," *Materials Today: Proceedings*, vol. 21, pp. 346–350, 2020. https://doi.org/10.1016/j.matpr.2019.05.460

[22] D. Bouras, M. Fellah, R. Barille *et al.*, "Properties of MZO/ceramic and MZO/glass thin layers based on the substrate's quality," *Optical and Quantum Electronics*, vol. 56, no. 1, 104, 2024. https://doi.org/10.1007/s11082-023-05778-6

[23] D. S. Mahjoob, A. A. Khalaf, and M. M. Hanon, "Forecasting cutting force by using artificial neural networks based on experiments of turning Aluminum," *International Journal of Mechanical Engineering and Robotics Research*, vol. 12, no. 6, 2023. doi: 10.18178/ijmerr.12.6.410-416

[24] M.R. Atia, M. Mokhtar, and J. Khalil, "An ANN parametric approach for the estimation of total production operation time," *Ain Shams Engineering Journal*, vol. 13, no. 2, 101579, 2022. https://doi.org/10.1016/j.asej.2021.09.006

[25] P. Dey and A. K. Das, "Steady flow over triangular extended solid attached to square cylinder—A method to reduce drag," *Ain Shams Engineering Journal*, vol. 6, no. 3, pp. 929–938, 2015. https://doi.org/10.1016/j.asej.2015.01.002

[26] S. Zhou, D. Chen, W. Cai *et al.*, Crowd modeling and simulation technologies," *ACM Transactions on Modeling and Computer Simulation (TOMACS)*, vol. 20, no. 4, pp. 1–35, 2010. https://doi.org/10.1145/1842722.1842725

[27] H. Bossel, *Modeling and Simulation*, AK Peters/CRC Press, 2018. https://doi.org/10.1201/9781315275574

[28] L. Zhang, L. Zhou, L. Ren *et al.*, "Modeling and simulation in intelligent manufacturing," *Computers in Industry*, vol. 112, 103123, 2019. https://doi.org/10.1016/j.compind.2019.08.004

[29] M. G. Cimino, F. Palumbo, G. Vaglini *et al.*, "Evaluating the impact of smart technologies on harbor's logistics via BPMN modeling and simulation," *Information Technology and Management*, vol. 18, no. 3, pp. 223–239, 2017. https://doi.org/10.1007/s10799-016-0266-4

[30] K. Z. Yang, A. Pramanik, A. Basak *et al.*, "Application of coolants during tool-based machining—A review," *Ain Shams Engineering Journal*, 101830, 2022. https://doi.org/10.1016/j.asej.2022.101830

[31] M. A. Taha, N. A. El-Mahallawy, R. M. Hammouda *et al.*, "Machinability characteristics of lead free-silicon brass alloys as correlated with microstructure and mechanical properties," *Ain Shams Engineering Journal*, vol. 3, no. 4, pp. 383–392, 2012. https://doi.org/10.1016/j.asej.2012.05.004

[32] K. Sambhav, A. Kumar, and S. K. Choudhury, "Mechanistic force modeling of single point cutting tool in terms of grinding angles," *International Journal of Machine Tools and Manufacture*, vol. 51, no. 10&11, pp. 775–786, 2011. https://doi.org/10.1016/j.ijmachtools.2011.06.007

[33] J. Patel, D. Panchal, H. Patel *et al.*, "Harmonic analysis of single point cutting tool with Multi-layer Passive Damping (MLPD) technique," *Materials Today: Proceedings*, vol. 44, pp. 625–628, 2021. https://doi.org/10.1016/j.matpr.2020.10.601

[34] R. Bhogal, M. Singh, and A. Madan, "Cutting force & thermal analysis during turning using ANSYS," *Materials Today: Proceedings*, vol. 56, pp. 3577–3584, 2022. https://doi.org/10.1016/j.matpr.2021.12.001

[35] R. Mishra, V. Dubey, R. K. Singh *et al.*, "A novel conjugate heat transfer approach to determine the temperature distribution in single-point cutting tool under different conditions," in *Proc. the Institution of Mechanical Engineers, Part E*, 2022. https://doi.org/10.1177/09544089221125633

[36] C. Choudhari, I. Bhisti, M. Choudhary *et al.*, "Vibrational analysis of single-point cutting tool for different tool material and nose radius using design of experiment," in *Proc. International Conference on Intelligent Manufacturing and Automation, Springer*, 2019, pp. 35–45. https://doi.org/10.1007/978-981-13-2490-1_4

[37] S. Pervaiz, I. Deiab, E. Wahba *et al.*, "A numerical and experimental study to investigate convective heat transfer and associated cutting temperature distribution in single point turning," *The International Journal of Advanced Manufacturing Technology*, vol. 94, no. 1, pp. 897–910, 2018. https://doi.org/10.1007/s00170-017-0975-9

[38] A. Kohli, V. Ghalagi, M. Divate *et al.*, "Heat analysis of single point cutting tool coated with different natural bio composite," *Journal of Physics: Conference Series, IOP Publishing*, 012186, 2020. doi: 10.1088/1742-6596/1706/1/012186

[39] A. Tripathi, P. Das, and T. Aggarwal, "Diminution of chatter vibration in single point cutting tool holder using Finite Element Analysis (FEA)," *Materials Today: Proceedings*, 2022. https://doi.org/10.1016/j.matpr.2022.04.423

[40] M. Nikam, A. Karulkar, A. Chowdhury *et al.*, "Performance of a single point cutting tool with textured surfaces: A Comparative study of different textured patterns," *Recent Advances in Manufacturing Processes and Systems*, *Springer*, pp. 777–790, 2022. https://doi.org/10.1007/978-981-16-7787-8_62

[41] M. Ozakpolor, C. Aliyegbenoma, and D. D. Olodu, "Prediction of cutting temperature in carbide cutting tool using finite element method," *International Advanced Researches and Engineering Journal*, vol. 5, no. 3, pp. 398–404, 2021. https://doi.org/10.35860/iarej.859488

[42] Y. Meng, J. Wei, J. Wei *et al.*, "An ANSYS/LS-DYNA simulation and experimental study of circular saw blade cutting system of mulberry cutting machine," *Computers and Electronics in Agriculture*, vol. 157, pp. 38–48, 2019. https://doi.org/10.1016/j.compag.2018.12.034

[43] J. Keuntje, S. Mrzljak, L. Gerdes *et al.*, "Macroscopic simulation model for laser cutting of carbon fibre reinforced plastics," *Procedia CIRP*, vol. 111, pp. 496–500, 2022. https://doi.org/10.1016/j.procir.2022.08.078

[44] A. Mir, X. Luo, K. Cheng *et al.*, "Investigation of influence of tool rake angle in single point diamond turning of silicon," *The International Journal of Advanced Manufacturing Technology*, vol. 94, no. 5, pp. 2343–2355, 2018. https://doi.org/10.1007/s00170-017-1021-7

[45] W. Lau, P. Venuvinod, and C. Rubenstein, "The relation between tool geometry and the Taylor tool life constant," *International Journal of Machine Tool Design and Research*, vol. 20, no. 1, pp. 29–44, 1980. https://doi.org/10.1016/0020-7357(80)90016-5

[46] K. Gok, H. Sari, A. Gok *et al.*, "Three-dimensional finite element modeling of effect on the cutting forces of rake angle and approach angle in milling," *The Institution of Mechanical Engineers, Part E: Journal of Process Mechanical Engineering*, 2017, vol. 231, no. 2, pp. 83–88. https://doi.org/10.1177/0954408915576698

[47] X. Guo, Y. Li, L. Cai *et al.*, "Effects of tool edge radius on chip formation during the micromachining of pure iron," *The International Journal of Advanced Manufacturing Technology*, vol. 108, no. 7, pp. 2121–2130, 2020. https://doi.org/10.1007/s00170-020-05528-y

[48] B. Liu, Z. Xu, C. Chen *et al.*, "Effect of tool edge radius on material removal mechanism of single-crystal silicon: Numerical and experimental study," *Computational Materials Science*, vol. 163, pp. 127–133, 2019. https://doi.org/10.1016/j.commatsci.2019.03.025

[49] V. P. Astakhov, "Basic definitions and cutting tool geometry, single point cutting tools," *Geometry of Single-point Turning Tools and Drills: Fundamentals and Practical Applications*, pp. 55–126, 2010. https://doi.org/10.1007/978-1-84996-053-3_2

[50] S. Dinesh, V. Vijayan, A. Parthiban *et al.*, "Modeling and optimization of machining parameters for turning of mild steel using single-point cutting tool made of P20 tool steel," *Advances in Industrial Automation and Smart Manufacturing*, pp. 285–295, 2021. https://doi.org/10.1007/978-981-15-4739-3_24

[51] M. Tauhiduzzaman and S. Veldhuis, "Effect of material microstructure and tool geometry on surface generation in single point diamond turning," *Precision Engineering*, vol. 38, no. 3, pp. 481–491, 2014. https://doi.org/10.1016/j.precisioneng.2014.01.002

[52] S. Atlati, A. Moufki, M. Nouari *et al.*, "Interaction between the local tribological conditions at the tool–chip interface and the thermomechanical process in the primary shear zone when dry machining the aluminum alloy AA2024–T351," *Tribology International*, vol. 105, pp. 326–333, 2017. https://doi.org/10.1016/j.triboint.2016.10.006

[53] T. T. Opoz and X. Chen, "Chip formation mechanism using finite element simulation," *Strojniški Vestnik-Journal of Mechanical* Engineering, vol. 62, no. 11, 2016. https://doi.org/10.5545/sv-jme.2016.3523

[54] N. Abukhshim, P. Mativenga, and M. A. Sheikh, "Heat generation and temperature prediction in metal cutting: A review and implications for high speed machining," *International Journal of Machine Tools and Manufacture*, vol. 46, no. 7–8, pp. 782–800, 2006. https://doi.org/10.1016/j.ijmachtools.2005.07.024

[55] Y. Bao, X. Zhang, S.-X. Lu *et al.*, "Investigation on the removal characteristics of single-point cutting high-volume fraction SiCp/Al composites," *The International Journal of Advanced Manufacturing Technology*, vol. 118, no. 3, pp. 881–894, 2022. https://doi.org/10.1007/s00170-021-07977-5

[56] D. Umbrello, S. Rizzuti, J. Outeiro *et al.*, "Hardness-based flow stress for numerical simulation of hard machining AISI H13 tool steel," *Journal of Materials Processing Technology*, vol. 199, no. 1–3, pp. 64–73, 2008. https://doi.org/10.1016/j.jmatprotec.2007.08.018

[57] S. Campocasso, G. Poulachon, S. Bissey-Breton *et al.*, "Towards cutting force evaluation without cutting tests," *CIRP Annals*, vol. 66, no. 1, pp. 77–80, 2017. https://doi.org/10.1016/j.cirp.2017.04.023

[58] H. Bharath and H. Shivashankar, "Evaluation of high temperature characteristics and tool life of high carbon and high chromium steel as a single point cutting tool," *Materials Today: Proceedings*, vol. 4, no. 9, pp. 10591–10595, 2017. https://doi.org/10.1016/j.matpr.2017.06.425

[59] M. Uthayakumar, G. Prabhakaran, S. Aravindan *et al.*, "Influence of cutting force on bimetallic piston machining by a Cubic Boron Nitride (CBN) tool," *Materials and Manufacturing Processes*, vol. 27, no. 10, pp. 1078–1083, 2012. https://doi.org/10.1080/10426914.2012.677913

[60] I. P. Okokpujie, O. M. Ikumapayi, U. C. Okonkwo *et al.*, "Experimental and mathematical modeling for prediction of tool wear on the machining of aluminium 6061 alloy by high speed steel tools," *Open Engineering*, vol. 7, no. 1, pp. 461–469, 2017. https://doi.org/10.1515/eng-2017-0053

[61] T. Baizeau, S. Campocasso, G. Fromentin *et al.*, "Effect of rake angle on strain field during orthogonal cutting of hardened steel with c-BN tools," *Procedia Cirp*, vol. 31, pp. 166–171, 2015. https://doi.org/10.1016/j.procir.2015.03.089

[62] K. Aydın, A. Akgün, Ç. Yavaş *et al.*, "Experimental and numerical study of cutting force performance of wave form end mills on gray cast iron," *Arabian Journal for Science and Engineering, vol.* 46, no. 12, pp. 12299–12307, 2021. https://doi.org/10.1007/s13369-021-05816-z